Research
Public Health—Article

Assessing the Effect of Global Travel and Contact Restrictions on Mitigating the COVID-19 Pandemic

Shengjie Lai [a,*], Nick W. Ruktanonchai [a,b,*], Alessandra Carioli [a], Corrine W. Ruktanonchai [a], Jessica R. Floyd [a], Olivia Prosper [c], Chi Zhang [d], Xiangjun Du [d], Weizhong Yang [e], Andrew J. Tatem [a,*]

[a] WorldPop, School of Geography and Environmental Science, University of Southampton, Southampton SO17 1BJ, UK
[b] Population Health Sciences, Virginia Tech, Blacksburg, VA 24061, USA
[c] Department of Mathematics, University of Tennessee, Knoxville, TN 37996, USA
[d] School of Public Health (Shenzhen), Sun Yat-sen University, Shenzhen 510275, China
[e] School of Population Medicine and Public Health, Chinese Academy of Medical Sciences & Peking Union Medical College, Beijing 100730, China

ARTICLE INFO

ABSTRACT

Travel restrictions and physical distancing have been implemented across the world to mitigate the coronavirus disease 2019 (COVID-19) pandemic, but studies are needed to understand their effectiveness across regions and time. Based on the population mobility metrics derived from mobile phone geolocation data across 135 countries or territories during the first wave of the pandemic in 2020, we built a metapopulation epidemiological model to measure the effect of travel and contact restrictions on containing COVID-19 outbreaks across regions. We found that if these interventions had not been deployed, the cumulative number of cases could have shown a 97-fold (interquartile range 79–116) increase, as of May 31, 2020. However, their effectiveness depended upon the timing, duration, and intensity of the interventions, with variations in case severity seen across populations, regions, and seasons. Additionally, before effective vaccines are widely available and herd immunity is achieved, our results emphasize that a certain degree of physical distancing at the relaxation of the intervention stage will likely be needed to avoid rapid resurgences and subsequent lockdowns.

1. Introduction

The coronavirus disease 2019 (COVID-19) pandemic has caused an evolving global public health and economic crisis [1–3]. Before effective vaccines are widely available to achieve herd immunity, the medical and public health communities have been reliant upon non-pharmaceutical interventions (NPIs) for mitigating the COVID-19 pandemic [4–6]. Travel and physical distancing interventions have been implemented across countries by quarantining geographic "hot spots" and minimizing physical contact between infectors and susceptible populations [7–10]. These interventions have aimed to suppress the peaks of the waves in this pandemic and delay virus's resurgence, protect healthcare capacity, and reduce the morbidity and mortality caused by COVID-19 [10–13].

The implementation of travel restrictions and physical distancing measures, together with other interventions, for example, large-scale testing, contact tracing, and personal hygiene behaviors, are likely to have substantially reduced transmission rates and flattened epidemic curves across countries in the first half of 2020 [7–9,14]. However, the global effectiveness of these travel and social contact restrictions remains unclear, due to the varying durations and intensities of these interventions conducted across regions and time [15,16]. Additionally, to minimize the socioeconomic impacts of lockdowns or travel restrictions, strategies for relaxing these interventions are also of importance to prevent resurgences and additional lockdowns. For example, China has moved past the first wave of the COVID-19 and lifted travel restrictions that were strictly implemented between late January and early March 2020 [17]. However, premature and sudden lifting of uncoordinated interventions could lead to a resurgence and an earlier secondary peak [18–21], such as the rapid resurgences and third lockdowns that have been occurring in Europe. An uncontrolled outbreak in one country may introduce transmission in

another country [12,22]. However, few studies have been conducted using quantitative measures of global travel and contact reductions to inform how and when social distancing measures should be implemented or lifted in the absence of a vaccine or effective treatment [18,19]. To answer these questions, the effectiveness of interventions and potential relaxation strategies across countries should be measured and assessed to guide ongoing and future COVID-19 or other pandemic responses [23].

Anonymized and aggregated human mobility data derived from mobile devices have been increasingly used to provide approximations of population-level travel patterns and physical contacts throughout the COVID-19 pandemic [24–26]. These data help refine interventions by providing timely information about changes in patterns of human mobility across space and time [27–30]. Here, we use population movement data to measure the intensity and timing of actual travel across 135 countries and territories throughout the first wave of the COVID-19 pandemic in 2020. A metapopulation transmission model was built to ① simulate COVID-19 spread across these countries, ② assess the relative effectiveness of travel and physical distancing interventions that were in place, and ③ examine various relaxation strategies. The potential numbers of age-specific severe and critical COVID-19 cases by population, region, and season were also estimated to help guide healthcare resource preparedness.

2. Methods

2.1. Mobile phone-derived travel and contact reductions

Two aggregated and anonymized population mobility datasets, obtained from Google and Baidu, were used to approximate measurements for the intensity of both travel and physical distancing interventions across space and time throughout the early stage of the COVID-19 pandemic.

2.1.1. Google data

The Google COVID-19 Aggregated Mobility Research Dataset contains anonymized mobility flows aggregated from users who have turned on their location history settings, which is off by default [31]. This is similar to the data used to show how busy certain types of places are in Google Maps—helping to identify when a local business tends to be the most crowded. The dataset contained aggregated flows of people between S2 cells from January 5 to May 30, 2020. Each S2 cell represents a quadrilateral on the surface of the planet and allows for efficient indexing of geographical data [32]. This dataset was analyzed by researchers at the University of Southampton, UK as per the terms of the data sharing agreement. Production of this anonymized and aggregated dataset has been detailed in previous studies [23,31,33,34].

A total of 134 countries, territories, or areas outside of Chinese mainland had domestic outflow data over the study period, and among them, 104 had international outflow data. The cumulative weekly outflows of each country were then divided by the number of origin S2 cells (each was calculated only once) that contained data from January 5 to May 30, 2020. This was done to account for any bias that may have been introduced by the increasing number of S2 cells discarded in order to protect the privacy of the decreasing number of travelers under travel restrictions.

To be comparable across countries and stages of the outbreak, the population movement data during the physical distancing interventions used to control COVID-19 were further standardized using "normal" mobility flows before the COVID-19 outbreaks. Asian countries/regions neighboring Chinese mainland implemented travel restrictions and physical distancing interventions earlier than other countries, and at an early stage of the outbreak.

Therefore, the domestic and international weekly outflows in seven Asian countries/regions (Hong Kong Special Administrative Region (SAR) of China, India, Japan, Republic of Korea, Singapore, Thailand, and Vietnam) during the period of January 26 to May 30, 2020 were standardized by the mean flows during the three weeks of January 5–25, 2020; all remaining 127 countries/regions' outflows since February 16, 2020 were standardized using the mean movements from January 5 to February 15, 2020 as a baseline.

2.1.2. Baidu data

To capture the changing population movement patterns in China during the COVID-19, the daily population mobility data at prefectural level (342 cities) in Chinese mainland in 2020 were obtained from Baidu's location-based services [35,36]. Baidu provides over seven billion positioning requests per day from people who use relevant mobile phone applications. The aggregated and de-identified daily outbound and inbound flows (travel index) for each prefecture-level city are publicly-available online. These data have been used to understand mobility patterns during the pandemic [35] and in previous studies [9,27]. To derive the country-level mobility data, we calculated the mean daily outflows across the country from January 5 to May 2, 2020. As Wuhan's lockdown and travel restrictions were enforced on January 23, 2020, the daily flows since January 23 were standardized by the mean outflows across Chinese mainland from January 5 to 22, 2020 to compare reductions in travel over time.

2.2. Estimating effective reproduction numbers

To account for variations in the transmissibility of severe acute respiratory syndrome coronavirus 2 (SARS-CoV-2) in different regions, we calculated the reproduction number (the average number of new infections associated with one infected person) by country/territory, before the travel and physical distancing interventions were implemented. This was then used to simulate COVID-19 transmission and assess the effectiveness of various intervention and relaxation scenarios across regions and time.

2.2.1. COVID-19 case data

We used country-specific daily counts of confirmed cases by date of report as of May 4, 2020 which were systematically collated by the European Centre for Disease Prevention and Control [37]. The numbers of cases by date of symptom onset reported in Chinese mainland as of May 2, 2020, were obtained from the Chinese National Health Commission [38] and an online resource of the Chinese Center for Disease Control and Prevention [39]. The epidemic curves in Hong Kong and Macao SARs, China were aggregated from individual case data obtained from the Centre for Health Protection, Department of Health, Hong Kong SAR, China [40] and the Bureau of Health, Macao SAR, China [41].

2.2.2. Adjusting for reporting delays

To parameterize COVID-19 transmission before travel and physical distancing interventions, we estimated the effective reproduction number (R_e) before these interventions were implemented by country or territory. For estimates of R_e that were made at the date of report, any changes and interventions in the time-varying parameters during the simulation of COVID-19 transmission were delayed due to the incubation period and reporting. In order to reduce the potential biases in estimates of R_e due to these delays, for a given country, we drew a sample of infection–onset–report delays from the posterior distributions of the incubation period and symptom-to-report period, to transform each observed reporting date into a sample infection date [42]. This resulted in 1000 samples of infection and onset date for each confirmed case. Then

we calculated R_e using the adjusted epidemic curve of daily case counts generated from the potential infection dates before implementing travel and physical distancing interventions. The distributions of incubation period (log-normal distribution with a mean of 5.2 d, 95% confidence interval (CI) 4.1–7.0 d) and the period from symptom onset to first medical visit/report (Weibull distribution with a mean of 5.8 d, 95% CI 4.3–7.5 d) were obtained from the epidemiological data at the early stage before the lockdown of Wuhan on January 23, 2020 [43].

2.2.3. Timing of travel and physical distancing interventions

The timing of various NPIs by country was derived from the government measures dataset which was systematically collated by the Assessment Capacities Project of the United Nations Office for the Coordination of Humanitarian Affairs [44]. This dataset assembled the measures implemented by governments worldwide in response to the COVID-19 pandemic. The collection of this dataset included secondary data reviewed from various data sources, and the available information fell into five categories: lockdowns, social distancing, (international) movement restrictions, public health measures, and social and economic measures. As our study focused on the travel and physical distancing interventions, we extracted data from the earliest dates of implementing lockdowns, physical distancing, and (international) movement restrictions, in each country/territory.

2.2.4. Estimating effective reproduction numbers

We preliminarily used an exponential growth (EG) method described in a previous study [45] to estimate the initial reproduction numbers before travel restrictions or lockdowns for each country/territory. We considered the period without travel and physical distancing interventions in the epidemic curve over which growth was exponential. An initial reproduction number was linked to the exponential growth rate, denoted by τ, at the early stage of the epidemic [46]. The exponential growth rate was measured by the per capita change in number of new infections. Poisson regression was used to estimate this parameter as the numbers of cases reported were integer values [47,48]. Therefore, we estimated the reproduction number, R_e, as

$$R_e = \frac{1}{M(-\tau)} \tag{1}$$

where M represents the discrete moment generating function that generates the time distribution. The generation of the time distribution is usually obtained from the interval between the time a person becomes infected and the infection time of his or her infector. Since the generation time cannot be calculated directly in our research, it was replaced with the serial interval generated from the Weibull distribution (a mean of 7, standard deviation (SD) of 3.4 d; constant across periods) which was derived from case data in Wuhan [43]. The "R0" package in the statistical software R [46] was used to estimate the R_e based on country-specific epidemic curves, adjusted for the incubation period and reporting delays as described above, before implementing the lockdown. If the lockdown date was unavailable, the period from the first case to the date of the maximum number of cases reported before May 2, 2020 was selected. To reduce the likelihood of spurious estimates for countries with limited transmission or case ascertainment, according to previous studies [49], we estimated the R_e for countries/territories with at least 500 cases reported, as of April 28, 2020. The R_e for these countries were used to estimate the initial reproduction numbers in the first wave of the pandemic. For countries with less than 500 cases, we used the median value of R_e (2.4, interquartile range (IQR) 2.0–2.8) estimated from other countries. In our COVID-19 simulations, for those countries/territories with an R_e value higher than 3, we substi-

tuted that R_e value with 3 to avoid any potential overestimation of transmission. Table S1 in Appendix A shows the R_e values by country or territory originally estimated in this study, with 95% CI provided.

2.3. Simulating COVID-19 transmission

To assess the effectiveness of various travel and physical distancing interventions on COVID-19 pandemic mitigation and resurgence, we used a metapopulation epidemiological model (coding for the model is available at https://github.com/wpgp/BEARmod) to simulate the COVID-19 spread across the 135 countries and territories for 13 months from December 1, 2019 to December 31, 2020.

2.3.1. Model framework

We simulated the spread of COVID-19 using a previously published epidemiological modeling framework called susceptible–exposed–infectious–removed (SEIR) to simulate the COVID-19 pandemic across Chinese mainland [9]. In this model, each country/territory was represented as a separate subpopulation (N) with its own susceptible (S), exposed (E), infected (I), and recovered/removed (R) populations. Based on a typical SEIR model, these stochastic infection processes within each country therefore approximated the following continuous-time deterministic model:

$$\frac{dS}{dt} = S - c \cdot \frac{S \cdot I}{N} \tag{2}$$

$$\frac{dE}{dt} = c \cdot \frac{S \cdot I}{N} - \varepsilon E \tag{3}$$

$$\frac{dI}{dt} = \varepsilon E - rI \tag{4}$$

$$\frac{dR}{dt} = rI \tag{5}$$

where t is for a particular moment, c is the travel and contact rate of each country, ε is the inverse of the average time spent exposed to the virus but not infectious, and r denotes the rate of infected people becoming noninfectious per day due to recovery, death, or removal by isolation.

2.3.2. Model parameterization

For each day within our simulations, infected people recovered or were removed at an average rate r, which was equal to the inverse of the average infectious period. Explicitly, a Bernoulli trial was incorporated for each infected person with the probability of recovering being $1 - e^{-r}$. The time lags from illness onset to diagnosis/reporting were used as proxies for the average infectious period, indicating the improved timeliness of case identification and isolation. Based on the information derived from confirmed cases in Wuhan and the first cases reported by county across Chinese mainland before and since Wuhan's lockdown on January 23, 2020 [9,50], the time differences between disease onset and reporting/isolation/quarantine used in the model decreased from an 11-day lag before the lockdown (or physical distancing if the date of lockdown was unavailable) to a 3-day lag following day 15 of the lockdown, with the lag decreasing every 2 d from lockdown day 1 to day 14. Following day 15 of interventions, we also added an extra 0.5 d to the 3-day lag to account for potential transmission by asymptomatic persons before illness onset [51]. Additionally, the model converted exposed individuals to infectious individuals by similarly incorporating a Bernoulli trial for each exposed individual, with the daily probability of becoming infectious being $1 - e^{-\varepsilon}$. For this, ε was calculated as the inverse of

the incubation period (5.2 d, 95% CI 4.1–7.0 d), which was estimated from case data in Wuhan [43].

The number of newly exposed individuals was calculated for each country based on the number of infectious individuals in the country and the average number of daily contacts an infectious individual had that potentially lead to disease transmission. We simulated the number of exposed individuals in a country on a given day through a random draw from a Poisson distribution for each infectious individual where the mean number of new infections per person was c. This was subsequently multiplied by the fraction of people in the country that were susceptible. The baseline daily contact rate, c, was calculated using the country-specific R_e, divided by the average delay (5.8 d, 95% CI 4.3–7.5 d) from onset to first medical visit that was estimated at the early stage of the outbreak [43]. To account for the impact of travel and contact restrictions, the daily contact rate, c, was weighted by the relative level of daily travel and contacts derived from Google and Baidu population mobility data within each country/territory. We assumed that no individual had existing immunity to COVID-19, and we did not include new susceptible individuals, or conversion of recovered individuals back to susceptible, as our simulation runs were not extended beyond 13 months. Corresponding country-level population data in 2020 for modelling were obtained from the United Nations[†].

2.3.3. Simulation run, validation, and sensitivity analysis

We initiated the simulated outbreak in each country/territory at the earliest date (Table S1) based on at least one case in the epidemic curves, adjusted by the reporting delays as detailed in Section 2.2.2. Considering the delay from infection to onset and report [52], we used December 1, 2019 as the initial date of simulation in China [27]. As in previous studies [9,53], the outbreak in each country was simulated and initiated by five infectious people at day 0. We initially found that five is the small number that can prevent stochastic extinction of the epidemic during the initial days of the simulation, and found no significant difference at the end of 2020 with simulation runs that initially started with five and seven infected people.

It should be noted that, as we needed sufficient days to start the simulation for generating the outbreak in each country or territory, the start dates of simulations used in this study were derived from reported case data are were only for the purposes of initializing and propagating the transmission. Therefore, this might not represent the actual timing of when the disease appeared in the country and caused the local transmission. In addition, the reported case data that we used do not have the information for classifying local and imported cases, and our model also did not consider the importation of pathogens via international population movements. Therefore, results from our study might underestimate the local transmission caused by imported cases.

Using this model, we simulated the transmission of COVID-19 in each country/territory using the parameters derived from the data before lockdowns as baseline scenarios. Then we compared the transmission of COVID-19 between scenarios with and without travel and physical distancing interventions, to assess the impact of these interventions. Our approach accounted for variance in recovery, exposure, and infection across many simulation runs (n = 1000), and assessed the effects and uncertainty of various intervention scenarios and the timing thereof, as well as the impact of relaxing these measures to guide future responses. Additionally, the estimates of the outbreak before and under travel and physical distancing interventions were compared with the reported number of COVID-19 cases across countries and time, as of June 1, 2020.

The reported epidemic curves adjusted for reporting delays were further compared to the patterns and epidemic curves estimated in this study. We also conducted a series of sensitivity analyses to understand the relative impact of changing epidemiological parameters on the estimates and uncertainties of intervention efficacy.

2.4. Estimating number of severe and critical cases

Based on the outputs of our COVID-19 transmission simulation, we further estimated the potential number of severe and critical cases that might need intensive health care. First, we obtained the age-specific severity risk from a cohort of 32 583 laboratory-confirmed patients in Wuhan, spanning the period from December 2019 through March 2020 [50]. A proportion (22.1%, 7139/32 325) of all confirmed cases with available data were severe or critical cases. The risk of severity increased with age, with 4.1% of those aged < 20 years, 12.1% of 20–39-year-olds, 17.4% of 40–59-year-olds, 29.6% of 60–79-year-olds, and 41.3% of those aged ≥ 80 years being severe or critical cases. We standardized the severity risk across these five age groups using population counts by age in Wuhan. Using the age-specific severity proportion ($S_{\mathrm{Wuhan},g}$) above and the number of cases ($I_{\mathrm{Wuhan},g}$, with 536, 5960, 12 269, 11 934, and 1884 cases, respectively) in each age group, g (0–19, 20–39, 40–59, 60–79, and ≥ 80 years of age) reported in Wuhan, combined with the country-specific number of cases (I_i) estimated by our simulations, we preliminarily estimated the number of severe and critical cases (C_i) in a country/territory, i, as below.

$$C_i = \sum C_{i,g} \tag{6}$$

$$C_{i,g} = I_i \cdot D_{i,g} \cdot S_{\mathrm{Wuhan},g} \tag{7}$$

where $D_{i,g} = \frac{I'_{i,g}}{\sum_{g} I'_{i,g}}$ and $I'_{i,g} = P_{i,g} \cdot \frac{I_{\mathrm{Wuhan},g}}{P_{\mathrm{Wuhan},g}}$. The $C_{i,g}$ was the estimate of severe and critical cases in a given age group, g, and country/territory, i. As we did not use age-structured transmission models to directly simulate the COVID-19 transmission by age group in each country/territory, we estimated the number of cases by age group using a country-/territory- and age-specific proportion ($D_{i,g}$). This was calculated from the age-specific incidence in Wuhan and standardized by the number of population counts by age group in Wuhan ($P_{\mathrm{wuhan},g}$) and study country/territory ($P_{i,g}$). The population data by age in Wuhan were obtained from the Wuhan Statistical Yearbook 2018 [54]. The age structures of the populations in the study countries or territories in 2020 were aggregated from the high-resolution gridded population count datasets (Appendix A Table S2) projected by the WorldPop[‡] [55]. R version 3.6.1 (R Foundation for Statistical Computing, Austria) was used to perform data collation and analyses in this study. Ethical clearance for collecting and using secondary population mobility data in this study was granted by the institutional review board of the University of Southampton, UK (No. 48002). All data were supplied and analyzed in an anonymous format, without access to personal identifying information.

3. Results

3.1. Intensity of travel and physical distancing interventions

Derived from two anonymized and aggregated mobility datasets obtained from Google and Baidu, population mobility across the 135 study countries and territories declined rapidly from mid-March 2020 due to the implementation of travel and physical

---

distancing interventions. Low levels of movement continued through April 2020 (Fig. 1). During the 10 weeks of March 22 to May 30, 2020, domestic travel decreased to a median of 59% (IQR 43%–73%) of levels seen before the interventions, with international travel down to 26% (IQR 12%–35%) of normal levels. However, the timing and intensity of these reductions in travel and physical contact differed. The reductions appeared earlier in countries that were initially strongly affected by COVID-19, for example, Italy, China, and other Asian countries or regions (Fig. 1). However, the decline in African countries occurred later and was less steep with higher residual travel and social contact levels, compared with other countries around the world (Fig. S1 in Appendix A). Population mobility gradually resumed in May 2020, with domestic travel back to a median of 69% (IQR 56%–80%) of normal levels and international travel recovering to 35% (IQR 15%–47%) during the four weeks from May 3 to 30, 2020 (Figs. 1(a) and (c)).

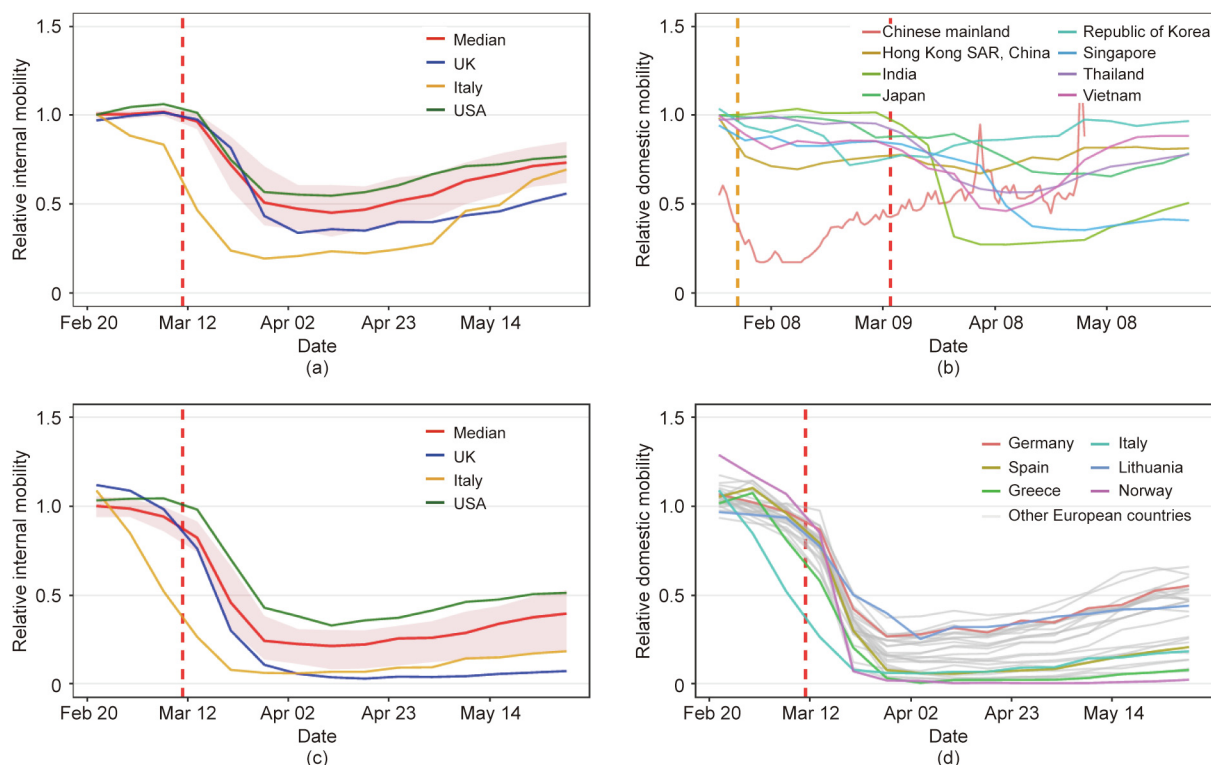### 3.2. Effects of global travel and contact reductions

We estimated that there were 15 million (IQR (11–20) million) COVID-19 cases under travel and physical distancing interventions across the 135 study countries or territories as of May 31, 2020. These interventions appear to have effectively suppressed the first wave of the pandemic, with 448 million (IQR (365–539) million) infections likely prevented in these areas as of May 31, 2020. Theoretically, without these interventions, the cumulative number of cases may have shown a 97-fold (IQR 79–116) increase as of May 31, 2020, and the peak of the pandemic might have occurred

around July–August 2020, with 51% (IQR 43%–60%) of the population having been infected across the study regions by the end of 2020. We estimated that if levels of travel and contact restrictions were to remain consistent through June 30, 2020, a total of 983 million (IQR (808–1169) million) infections would have been prevented by that date, and only 20 million (IQR (15–27) million) cases might have developed.
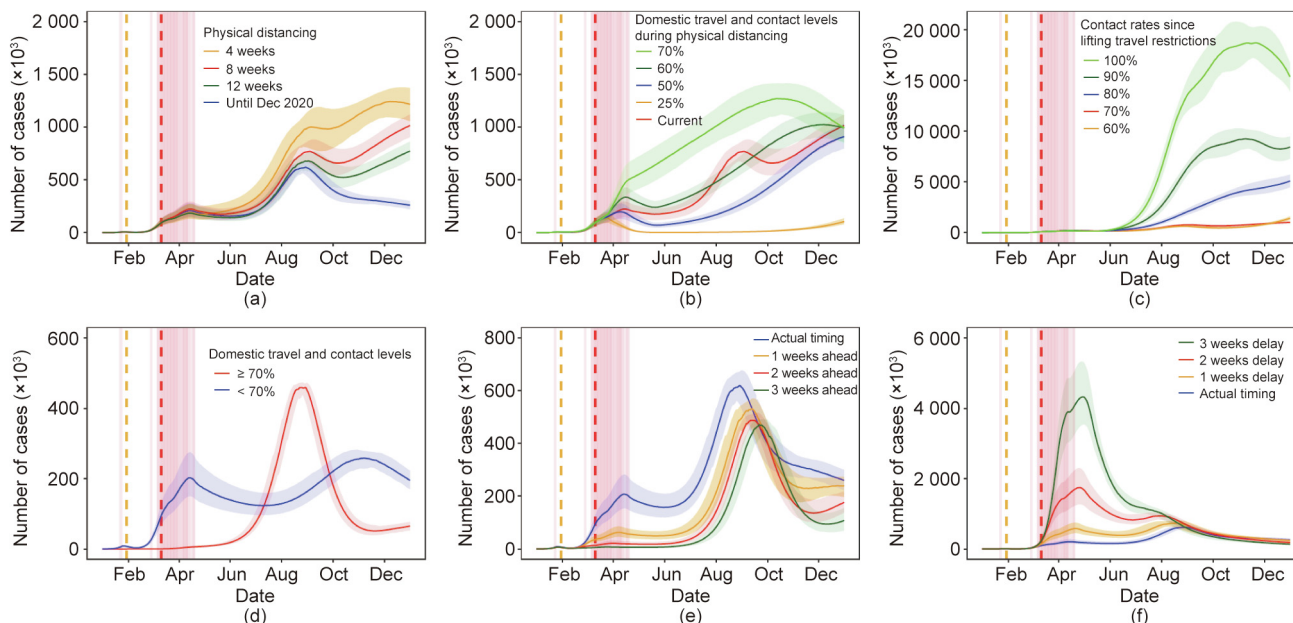
The timing of interventions is critical (Fig. 2). The World Health Organization (WHO) declared the COVID-19 outbreak a Public Health Emergency of International Concern on January 30, 2020 [1]. We estimated that, if all travel and physical distancing interventions put in place since February 23, 2020, one month after the lockdown of Wuhan City, had been implemented one, two, or three weeks earlier across the study regions outside of Chinese mainland, the number of COVID-19 cases by May 31, 2020, would have been dramatically reduced by 67% (IQR 55%–76%), 87% (IQR 81%–90%), or 95% (IQR 92%–96%), respectively (Fig. 2(e)). If, on the other hand, these interventions had been implemented one, two, or three weeks later than they were, the case count by the end of May, 2020, would have been 2.5-fold (IQR 1.9–3.3), 7.2-fold (IQR 5.3–9.3), or 16.4-fold (IQR 13.2–20.1) higher, respectively (Fig. 2(f)).

3.3. Impacts of various intervention and relaxation scenarios

Compared with the 4-week travel and physical distancing interventions, the 8-week and 12-week interventions were estimated to further reduce cases by 25% (IQR 20%–30%) and 39% (IQR 32%–

Fig. 1. Changing patterns of domestic and international population movements across countries or territories, as of May 30, 2020. (a) Domestic weekly movements within 127 countries or territories, with movements from January 5 to February 15, 2020 as a reference; (b) domestic population movements within eight Asian countries/regions (the daily mobility within Chinese mainland from January 23 to May 2, 2020 was derived from Baidu location-based data, standardized by averaged travel flow from January 5 to 22 before Wuhan's lockdown on January 23, 2020, and all other country or region curves were derived from weekly Google location history data, with movements from January 5 to 25 as a reference); (c) relative international outflows from 104 countries with available international mobility data; (d) relative international outflows from all European countries (the weekly international mobility measures, derived from Google data, took movements from January 5 to February 15 as a reference). The orange and red vertical dashed lines indicate the dates the World Health Organization (WHO) declared COVID-19 a Public Health Emergency of International Concern and a pandemic, respectively. The median (red line) and interquartile range (pink areas) are provided in (a) and (c), with the curves of Italy, the UK, and the USA presented. Each curve in (b) and (d) represents the relative travel pattern of a country or territory.

Fig. 2. Estimated epidemic curves of COVID-19 under different intervention scenarios across 135 countries or territories in 2020. (a) Implementing travel and physical distancing interventions during various periods (the median and interquartile ranges of estimates are shown); (b) 8-week interventions with various levels of travel and contact rates (in panels (a) and (b), the travel and contact levels after relaxing interventions were assumed to be 70% of normal level before the outbreaks, if the travel and contact rates in a country or territory were lower than 70%); (c) scenarios of various travel and contact rates after lifting 8-week interventions; (d) the estimated epidemic curves under interventions up until December 31, 2020 based on travel and contact levels by May 2, 2020: 14 countries/territories with travel and contact rates higher than or equal to 70%, and 121 countries/territories with the rate less than 70% at any week; (e) estimated epidemic curves under interventions implemented earlier than actual timing, under the scenario of interventions implemented by December 31, 2020; (f) estimated epidemic curves under interventions implemented later than actual timing, under the scenario of interventions implemented up until December 31, 2020. The orange and red vertical dashed lines indicate the dates the WHO declared COVID-19 a Public Health Emergency of International Concern and a pandemic, respectively. The pink vertical lines indicate the dates that lockdown/physical distancing measures were implemented by each country or territory.

45%), respectively, by December 31, 2020. However, if the travel and contact levels as of May 2, 2020 continued through the end of 2020, they would have only reduced the number of cases by 40% (IQR 33%–46%) further as of December 31, 2020. This figure is compared to estimates of an 8-week intervention and maintaining travel and contact rates at 70% of their normal levels after relaxing interventions (Fig. 2(a) and Appendix A Fig. S2). If a strict 8-week intervention could be in place across all regions in which there was only 25% of normal travel and contact rates, COVID-19 could be significantly suppressed to a relatively low level of daily new cases (median 4155, IQR 2555–7364) from May through September 2020, without a resurgence before October 2020 (Fig. 2(b)).

We further assessed the potential effects of various travel and contact rates after easing interventions. We found that, relaxing the interventions would result in an increase in the number of cases, and a complete cancellation of travel and physical distancing interventions would lead to a rapid resurgence of COVID-19 (Fig. 2 (c)). If the physical distancing intensity were maintained at 70% of normal levels or lower after relaxing interventions, countries might significantly delay the next wave and reduce its peak. However, due to the heterogeneity of intensities and extents in interventions among countries, we estimated that, in countries with weak travel and physical distancing interventions (travel and contact levels being higher or equal to 70% of normal levels), a relatively high proportion of populations (median 14%, IQR 11%–16%) might be infected by the end of 2020 (Fig. 2(d)). In contrast, other countries with more intensive measures would only have 0.9% (IQR 0.7%–1.1%) of their populations being infected by that date. These differences in interventions would result in temporal and spatial heterogeneity of COVID-19 across the world (Appendix A Fig. S3).
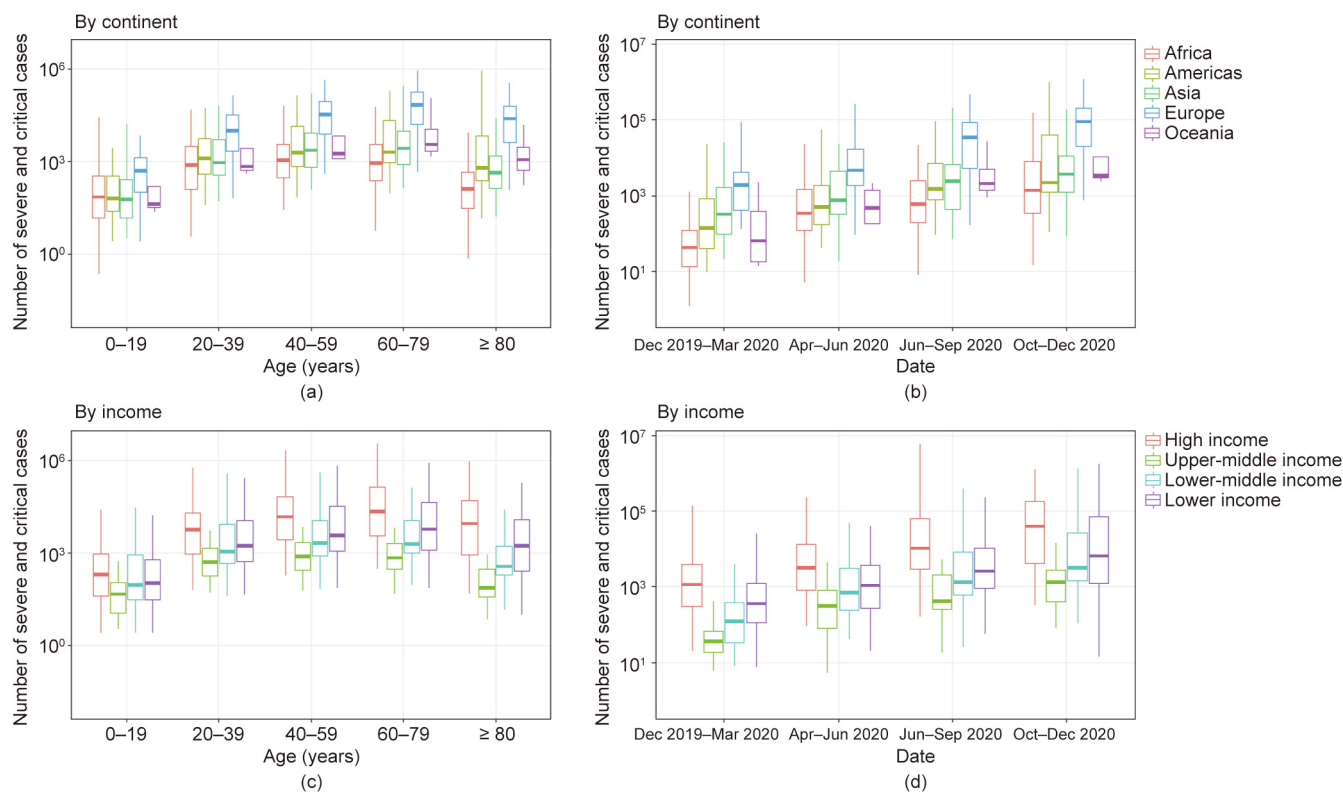
Based on our simulations of COVID-19's transmission under the 8-week travel and physical distancing interventions, the age struc-

ture of the population in each country/territory in 2020 [37], and the age-specific severity risk of confirmed COVID-19 cases reported from Wuhan [29], we estimated that a total of 0.9 million (IQR (0.6–1.2) million) cases as of March 31, 2020, would have been severe and critical cases, with a potential cumulative number of 33 million (IQR (28–39) million) severe and critical cases by the end of 2020. Substantial variations in severe and critical infections might be seen across populations, continents, income groups, and seasons (Fig. 3 [50,55] and Appendix A Figs. S4–S6).

We validated our model and outputs using reported case numbers across regions and periods as of June 1, 2020 (Fig. 4), with a series of sensitivity analyses conducted to help better understand the effectiveness of travel and physical distancing interventions under various settings (Appendix A Figs. S7–S11). Generally, the overall correlation between the number of estimated cases and the reported number by country or territory was significant ($p < 0.001$, $R^2 = 0.69$), with high correlations also found before ($p < 0.001$, $R^2 = 0.83$) and since ($p < 0.001$, $R^2 = 0.67$) the implementation of travel and physical distancing interventions. The estimated epidemic curves of the first wave in this pandemic were also consistent with reported data ($p < 0.001$, $R^2 = 0.91$) (Fig. 4(d)).

4. Discussion

The COVID-19 pandemic has led to an unprecedented number of travel restrictions and physical distancing interventions implemented around the world. Using aggregated and anonymized population mobility data derived from time- and space-explicit mobile phone data, our study quantified the role that travel and contact interventions had in mitigating the first wave of the pandemic across multiple countries. We found that since mid-March 2020, global population movements dramatically declined and remained

Fig. 3. Estimates of severe and critical COVID-19 cases in 135 countries or territories. (a) Estimates by age and continent; (b) estimates by season and continent; (c) estimates by age and income classification of each country or territory (low income was less than 1026 USD·a^{-1} per capita; lower-middle income was from 1026 to 3995 USD·a^{-1} per capita; upper-middle income was from 3996 to 12 375 USD·a^{-1} per capita; high income was higher than 12 375 USD·a^{-1} per capita); (d) estimates by season and income classification of each country or territory. The estimates were based on the scenario of 8-week travel and physical distancing interventions as of May 30, 2020. If the travel and contact rates in a country or territory were lower than 70% of normal levels before the outbreak, the rates were assumed to return to 70% after relaxing the interventions. The estimates of severe and critical infections were preliminarily based on the age structures of populations in each country/territory in 2020 [55] and the age-specific severity risk of confirmed COVID-19 cases reported from Wuhan [50].
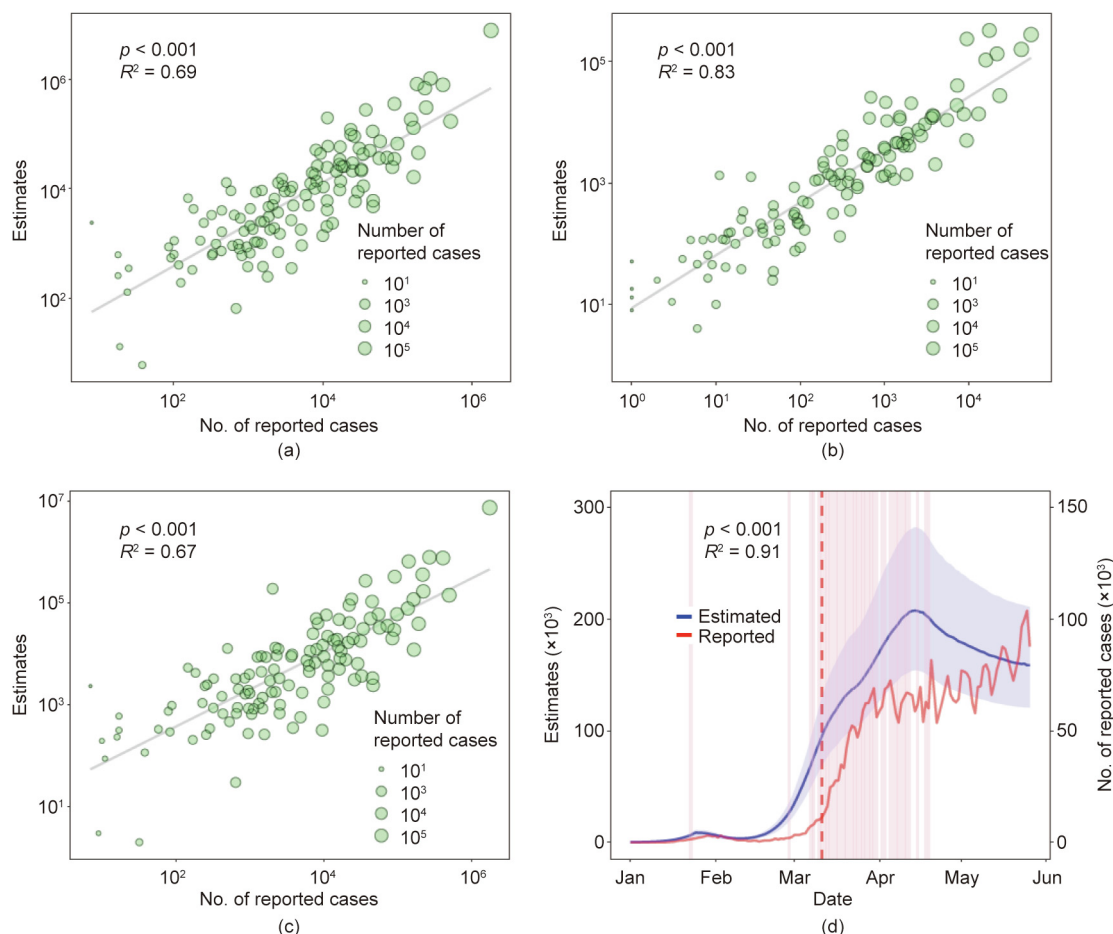
at low levels in April 2020, but gradually recovered in May 2020. These multi-nation, aggressive, and continuous measures played a significant role in suppressing and containing the pandemic in the first half of 2020, and likely prevented a large number of cases, in turn alleviating the pressure on medical and public health services in areas where COVID-19 has spread in the community. Ultimately, these early interventions likely helped to delay subsequent waves of the pandemic, stalling for global preparation and response, and increasing the potential for the development of vaccines and therapeutics that could be used in later stages.

The effectiveness of travel restrictions and physical distancing measures in slowing down COVID-19 transmission, however, hinged on the reduction in the number of contacts between infected individuals and healthy individuals, and between population groups with high rates of transmission and population groups with no or a low rates of transmission [10]. We found that the timing and intensity of physical distancing interventions in countries were not fully synchronized; therefore, the ability of these strategies to contain or mitigate the COVID-19 outbreak also differed. Due to this, the effects of the interventions manifest differently across regions and seasons, especially in regions with uncoordinated interventions and in low-income countries with weak prevention and control capabilities [56]. The travel and contact restrictions have slowed, but have not fully contained the outbreaks across the world [57], leading to ongoing resurgences and second or third lockdowns in many countries in 2020 and 2021.

At the end of April 2020, in hopes of reducing the human and economic impacts of social distancing measures, countries were gradually implementing exit strategies from these interventions

and formulating their next response to the pandemic. We found, however, that immediately lifting travel and physical distancing measures made a second wave of outbreaks inevitable, which was shown by our simulations and the reported data. Similar results have also been seen in previous modelling work [18,19]. Moreover, the effectiveness of restrictions to both global travel and physical contact varied by the duration of interventions, the intensity of physical distancing, and the travel and contact rates after relaxation of the interventions. Before the herd immunity against COVID-19 is achieved in populations, a certain degree of physical distancing, in parallel with early case detection, diagnosis, reporting and (self-)isolation, should be maintained to avoid a rapid resurgence [9]. In addition, if immunity is not permanent, periodic transmission, for example, annual cycle, will likely occur [19], and physical distancing interventions will again become necessary.

Several limitations in our study should be noted. First, the mobile phone data used in this study were limited to smartphone users who had opted into relevant product features. These data might not be representative of the population as a whole, and their representativeness might vary by location. Importantly, these limited data were subject to differential privacy algorithms, designed to protect user anonymity and obscure fine detail. Moreover, comparisons across rather than within locations could only be descriptive since regions differ in substantial ways. Second, the accuracy of our model relied on accurate estimates of R_e and other epidemiological parameters derived from reported case data. The quality of reported data and epidemiologic features of COVID-19 likely differed across countries/regions [58–60] due to varying case

Fig. 4. Comparing the estimated and reported numbers of COVID-19 cases across 135 countries or territories. (a) Estimates versus reported case counts by country/territory; (b) estimates versus reported numbers of cases before implementing lockdown/physical distancing measures; (c) estimates versus reported case counts after implementing lockdown/physical distancing measures; (d) estimated versus reported epidemic curves. The median and interquartile range of estimates are provided here. The reported case counts were obtained from European Centre for Disease Prevention and Control, as of June 1, 2020. To be comparable between estimated and reported data, time series of daily reported cases were moved back six days to account for the delay from illness onset to reporting. The red vertical dashed line indicates the date of COVID-19 pandemic declared by the WHO. The pink vertical lines indicate the dates of lockdown/nationwide physical distancing measures implemented by each country/territory. The Pearson's correlations between estimated and reported case numbers are presented with the p values of two-sided t-test.

definitions, diagnosis and surveillance capacity, population demographics, and other factors [61]. Third, we assumed the observed travel and contact reductions had similar effects in minimizing exposure risk of COVID-19 across space and time. The impact of physical distancing might, however, vary between urban and suburban or rural areas with different population densities. Fourth, many other factors might also contribute to COVID-19 spread, resurgence, containment, or mitigation. For example, our simulations did not specify the contributions of pre-symptomatic transmission, the presence of other NPIs such as using face masks, hand washing, and other preventive measures at community, family and individual levels [62], or the potential continuous importations of the virus via international travel, and the seasonal impacts of climatic factors that might have had a limited role in the early COVID-19 pandemic [63]. Future research is necessary to reveal the effects of travel restrictions and social distancing as well as other measures at national and international levels and at community, family, and individual levels over time [15,16]. Lastly, our preliminary estimates of the number of severe and critical cases by age assumed similarity in the severity of cases that were observed in Wuhan [64], and did not account for the individual characteristics, for example, comorbidities, contact, and mixing patterns [65], or country-specific healthcare capacity that varies widely across regions and may have influenced the risk of serious disease. Addi-

tionally, the estimated infections of severe and critical cases varied across age groups, continents, income groups, and seasons, indicating that further studies are needed to assess the impact of socioeconomic differences and demographic heterogeneities on COVID-19 for tailoring and adjusting response strategies in different populations and regions.

Viruses do not respect national borders, yet our societies are so deeply interconnected that the actions of one government can have rapid and profound global impacts. Our study serves to quantify important metrics of travel and physical distancing interventions, suggesting their potential effectiveness across the globe to improve international strategies and guiding national, regional, and global future responses to prioritize limited resources and strengthen healthcare capacity. Countries vary widely in terms of their ability to prevent, detect, and respond to outbreaks [66], and many low- and middle-income countries might not be able to provide sufficient access to health care resources in the face of a rapidly spreading infectious disease, such as COVID-19 [67]. For the time being, therefore, travel and physical distancing measures are critical tools in mitigating the impacts of the COVID-19 pandemic. Although COVID-19 vaccines have been rolled out in many countries, some levels of NPIs may be still required for considerably longer to prevent rapid resurgences and additional lockdowns [68,69]. Given the improving access of timely anonymized population movement

data for supporting COVID-19 mitigation across the globe [31], the potential exists to monitor and assess the effectiveness of travel and physical distancing interventions to inform strategies specifically against future waves of the COVID-19 pandemic as well as other infectious diseases in the future.

Acknowledgments

Author's contribution

Shengjie Lai designed the research. Shengjie Lai, Nick W. Ruktanonchai, and Olivia Prosper built the model. Shengjie Lai ran simulations and carried out analyses. Alessandra Carioli, Corrine W. Ruktanonchai, and Jessica R. Floyd provided technical support. Nick W. Ruktanonchai, Alessandra Carioli, Corrine W. Ruktanonchai, and Jessica R. Floyd helped with data curation. Alessandra Carioli collated the age-structure data of populations. Chi Zhang and Xiangjun Du collated Baidu mobility aggregated dataset. Olivia Prosper, Chi Zhang, Xiangjun Du, and Weizhong Yang did not access to the Google data used in this study. Shengjie Lai wrote the first draft of manuscript. Shengjie Lai, Nick W. Ruktanonchai, Alessandra Carioli, Corrine W. Ruktanonchai, Jessica R. Floyd, Olivia Prosper, Chi Zhang, Xiangjun Du, Weizhong Yang, and Andrew J. Tatem commented on and edited the manuscript.

Compliance with ethics guidelines

Shengjie Lai, Nick W. Ruktanonchai, Alessandra Carioli, Corrine W. Ruktanonchai, Jessica R. Floyd, Olivia Prosper, Chi Zhang, Xiangjun Du, Weizhong Yang, and Andrew J. Tatem declare that they have no conflict of interest or financial conflicts to disclose.

Data and materials availability

Code for the model simulations is available at the following GitHub repository: https://github.com/wpgp/BEARmod. The data on COVID-19 cases and interventions reported by country are available from the data sources listed in Materials and Methods. The parameters and population data for running simulations and estimating the severity are listed in Appendix A Tables S1 and S2. The population movement data obtained from Baidu are publicly available online at: https://qianxi.baidu.com/. The Google COVID-19 Aggregated Mobility Research Dataset used for this study is available with permission from Google LLC.

Ethical approval

Ethical clearance for collecting and using secondary population mobility data in this study was granted by the institutional review board of the University of Southampton (No. 48002). All data were supplied and analyzed in an anonymous format, without access to personal identifying information.

Appendix A. Supplementary data

Supplementary data to this article can be found online at https://doi.org/10.1016/j.eng.2021.03.017.

References

[1] Coronavirus disease (COVID-19) pandemic [Internet]. Geneva: World Health Organization; 2020 [cited 2020 Feb 29]. Available from: https://www.who.int/emergencies/diseases/novel-coronavirus-2019.
[2] Bonaccorsi G, Pierri F, Cinelli M, Flori A, Galeazzi A, Porcelli F, et al. Economic and social consequences of human mobility restrictions under COVID-19. Proc Natl Acad Sci USA 2020;117(27):15530–5.
[3] Yang J, Li J, Lai S, Ruktanonchai CW, Xing W, Carioli A, et al. Uncovering two phases of early intercontinental COVID-19 transmission dynamics. J Travel Med 2020;27(8):taaa200.
[4] Walker PGT, Whittaker C, Watson OJ, Baguelin M, Winskill P, Hamlet A, et al. The impact of COVID-19 and strategies for mitigation and suppression in low- and middle-income countries. Science 2020;369(6502):413–22.
[5] Flaxman S, Mishra S, Gandy A, Unwin HJT, Mellan TA, Coupland H, et al. Estimating the effects of non-pharmaceutical interventions on COVID-19 in Europe. Nature 2020;584(7820):257–61.
[6] Hu M, Lin H, Wang J, Xu C, Tatem AJ, Meng B, et al. The risk of COVID-19 transmission in train passengers: an epidemiological and modelling study. Clin Infect Dis 2020.
[7] Koo JR, Cook AR, Park M, Sun Y, Sun H, Lim JT, et al. Interventions to mitigate early spread of SARS-CoV-2 in Singapore: a modelling study. Lancet Infect Dis 2020;20(6):678–88.
[8] Cowling BJ, Ali ST, Ng TWY, Tsang TK, Li JCM, Fong MW, et al. Impact assessment of non-pharmaceutical interventions against coronavirus disease 2019 and influenza in Hong Kong: an observational study. Lancet Public Health 2020;5(5):e279–88.
[9] Lai S, Ruktanonchai NW, Zhou L, Prosper O, Luo W, Floyd JR, et al. Effect of non-pharmaceutical interventions to contain COVID-19 in China. Nature 2020;585 (7825):410–3.
[10] European Centre for Disease Prevention and Control. Considerations relating to social distancing measures in response to COVID-19—second update. [Internet]. Stockholm: European Centre for Disease Prevention and Control; 2020 [cited 2020 Apr 27]. Available from: https://www.ecdc.europa.eu/sites/default/files/documents/covid-19-social-distancing-measuresg-guide-second-update.pdf.
[11] Fong MW, Gao H, Wong JY, Xiao J, Shiu EYC, Ryu S, et al. Nonpharmaceutical measures for pandemic influenza in nonhealthcare settings–social distancing measures. Emerg Infect Dis 2020;26(5):976–84.
[12] Chinazzi M, Davis JT, Ajelli M, Gioannini C, Litvinova M, Merler S, et al. The effect of travel restrictions on the spread of the 2019 novel coronavirus (COVID-19) outbreak. Science 2020;368(6489):395–400.
[13] Tian H, Liu Y, Li Y, Wu CH, Chen B, Kraemer MUG, et al. An investigation of transmission control measures during the first 50 days of the COVID-19 epidemic in China. Science 2020;368(6491):638–42.
[14] Zhang J, Litvinova M, Liang Y, Wang Y, Wang W, Zhao S, et al. Changes in contact patterns shape the dynamics of the COVID-19 outbreak. Science 2020;368(6498):1481–6.
[15] Haug N, Geyrhofer L, Londei A, Dervic E, Desvars-Larrive A, Loreto V, et al. Ranking the effectiveness of worldwide COVID-19 government interventions. Nat Hum Behav 2020;4(12):1303–12.
[16] Brauner JM, Mindermann S, Sharma M, Johnston D, Salvatier J, Gavenčiak T, et al. Inferring the effectiveness of government interventions against COVID-19. Science 2021;371(6531):eabd9338.
[17] Maier BF, Brockmann D. Effective containment explains subexponential growth in recent confirmed COVID-19 cases in China. Science 2020;368 (6492):742–6.
[18] Leung K, Wu JT, Liu Di, Leung GM. First-wave COVID-19 transmissibility and severity in China outside Hubei after control measures, and second-wave scenario planning: a modelling impact assessment. Lancet 2020;395(10233):1382–93.
[19] Kissler SM, Tedijanto C, Goldstein E, Grad YH, Lipsitch M. Projecting the transmission dynamics of SARS-CoV-2 through the postpandemic period. Science 2020;368(6493):860–8.
[20] Prem K, Liu Y, Russell TW, Kucharski AJ, Eggo RM, Davies N, et al. The effect of control strategies to reduce social mixing on outcomes of the COVID-19 epidemic in Wuhan, China: a modelling study. Lancet Public Health 2020;5(5): e261–70.
[21] López L, Rodó X. The end of social confinement and COVID-19 re-emergence risk. Nat Hum Behav 2020;4(7):746–55.
[22] Pang X, Ren L, Wu S, Ma W, Yang J, Di L, et al. Cold-chain food contamination as the possible origin of COVID-19 resurgence in Beijing. Natl Sci Rev 2020;7 (12):1861–4.
[23] Ruktanonchai NW, Floyd JR, Lai S, Ruktanonchai CW, Sadilek A, Rente-Lourenco P, et al. Assessing the impact of coordinated COVID-19 exit strategies across Europe. Science 2020;369(6510):1465–70.
[24] Sills J, Buckee CO, Balsari S, Chan J, Crosas M, Dominici F, et al. Aggregated mobility data could help fight COVID-19. Science 2020;368(6487):145–6.
[25] Lai S, Farnham A, Ruktanonchai NW, Tatem AJ. Measuring mobility, disease connectivity and individual risk: a review of using mobile phone data and mHealth for travel medicine. J Travel Med 2019;26(3):taz019.

[26] Ruktanonchai NW, Ruktanonchai CW, Floyd JR, Tatem AJ. Using google location history data to quantify fine-scale human mobility. Int J Health Geogr 2018;17(1):28.

[27] Lai S, Bogoch I, Ruktanonchai N, Watts A, Lu X, Yang W, et al. Assessing spread risk of novel coronavirus within and beyond China, January–April 2020: a travel network-based modelling study. 2020. medRxiv:2020.02.04.20020479.

[28] Wu JT, Leung K, Leung GM. Nowcasting and forecasting the potential domestic and international spread of the 2019-nCoV outbreak: a modelling study. Lancet 2020;395(10225):689–97.

[29] Aktay A, Bavadekar S, Cossoul G, Davis J, Damien Desfontaines, Fabrikant A, et al. Google COVID-19 community mobility reports: anonymization process description (version 1.0). 2020. arXiv:2004.04145.

[30] Oliver N, Lepri B, Sterly H, Lambiotte R, Deletaille S, De Nadai M, et al. Mobile phone data for informing public health actions across the COVID-19 pandemic life cycle. Sci Adv 2020;6(23):eabc0764.

[31] Bassolas A, Barbosa-Filho H, Dickinson B, Dotiwalla X, Eastham P, Gallotti R, et al. Hierarchical organization of urban mobility and its connection with city livability. Nat Commun 2019;10(1):4817.

[32] Ardalan MR, Shoja MM. Rapidly progressive glomerulonephritis in a patient with brucellosis. Nephrol Dial Transplant 2006;21(6):1743–4.

[33] Rader B, Scarpino SV, Nande A, Hill AL, Adlam B, Reiner RC, et al. Crowding and the shape of COVID-19 epidemics. Nat Med 2020;26(12):1829–34.

[34] Wilson R, Zhang CY, Lam W, Desfontaines D, Simmons-Marengo D, Gipson B. Differentially private SQL with bounded user contribution. 2019. arXiv:1909.0191.

[35] Baidu Migration. Popular places to relocate during the Spring Festival travel season (destination) [Internet]. Beijing: Baidu; 2020 [cited 2020 Feb 8]. Available from: https://qianxi.baidu.com/.

[36] Lai S, Wangteeraprasert T, Sermkaew T, Nararak O, Binsard S, Phanawadee M, et al. Evaluation of three main tuberculosis case reporting systems in Satun Province, Thailand, 2011. Outbreak Surveill Invest Rep 2014;7(3):16–23.

[37] Download today's data on the geographic distribution of COVID-19 cases worldwide [Internet]. Stockholm: European Centre for Disease Prevention and Control; 2020 [cited 2020 May 2]. Available from: https://www.ecdc.europa.eu/en/publications-data/download-todays-data-geographic-distribution-covid-19-cases-worldwide.

[38] [COVID-19 pandemic daily report] [Internet]. Beijing: National Health Commission of China; 2021 [cited 2021 Jan 10]. Available from: http://www.nhc.gov.cn/xcs/yqtb/list_gzbd.shtml. Chinese.

[39] The knowledge center for China's experiences in response to COVID-19: prevention and control measure of COVID-19 in China [Internet]. Beijing: Chinese Center for Disease Control and Prevention; 2020 [cited 2020 Apr 25]. Available from: https://covid19.alliancebrh.com/covid19en/c100037/202004/abfdd96da7f340fe9e4ca8a063b0d2a6/files/4b92097245cb48a391ea4f6b40707ae5.pdf.

[40] Data in coronavirus disease (COVID-19) [Internet]. Hong Kong: Centre for Health Protection HKS; 2020 [cited 2020 Apr 28]. Available from: https://data.gov.hk/en-data/dataset/hk-dh-chpsebcddr-novel-infectious-agent.

[41] Special webpage against epidemics [Internet]. Beijing: Chinese Center for Disease Control and Prevention; 2020 [cited 2020 Apr 28]. Available from: https://www.ssm.gov.mo/apps1/PreventCOVID-19/en.aspx#clg17046.

[42] Yang WZ, Lan YJ, Lyu W, Leng ZW, Feng LZ, Lai SJ, et al. Establishment of multi-point trigger mechanism and multi-channel surveillance mechanism for intelligent early warning of infectious diseases in China. Chin J Epidemiol 2020;41(11):1753–7. Chinese.

[43] Li Q, Guan X, Wu P, Wang X, Zhou L, Tong Y, et al. Early transmission dynamics in Wuhan, China, of novel coronavirus-infected pneumonia. N Engl J Med 2020;382(13):1199–207.

[44] data.humdata.org [Internet]. New York: United Nations Office for the Coordination of Humanitarian Affairs; 2020 [cited 2020 Apr 28]. Available from: https://data.humdata.org/dataset/acaps-covid19-government-measures-dataset.

[45] Wallinga J, Lipsitch M. How generation intervals shape the relationship between growth rates and reproductive numbers. Proc Biol Sci 2007;274(1609):599–604.

[46] Obadia T, Haneef R, Boelle PY. The R0 package: a toolbox to estimate reproduction numbers for epidemic outbreaks. BMC Med Inform Decis Mak 2012;12(1):147.

[47] Boëlle PY, Bernillon P, Desenclos JC. A preliminary estimation of the reproduction ratio for new influenza A (H1N1) from the outbreak in Mexico, March–April 2009. Euro Surveill 2009;14(19):19205.

[48] Hens N, Van Ranst M, Aerts M, Robesyn E, Van Damme P, Beutels P. Estimating the effective reproduction number for pandemic influenza from notification data made publicly available in real time: a multi-country analysis for influenza A/H1N1v 2009. Vaccine 2011;29(5):896–904.

[49] Abbott S, Hellewell J, Thompson RN, Sherratt K, Gibbs HP, Bosse NI, et al. Estimating the time-varying reproduction number of SARS-CoV-2 using national and subnational case counts. Wellcome Open Res 2020;5:112.

[50] Pan A, Liu L, Wang C, Guo H, Hao X, Wang Q, et al. Association of public health interventions with the epidemiology of the COVID-19 outbreak. JAMA 2020;323(19):1915–23.

[51] Huang C, Zhang X, Zhang X, Wei Z, Zhang L, Xu J, et al. Rapid asymptomatic transmission of COVID-19 during the incubation period demonstrating strong infectivity in a cluster of youngsters aged 16–23 years outside Wuhan and characteristics of young patients with COVID-19: a prospective contact-tracing study. J Infect 2020;80(6):e1–13.

[52] Li R, Pei S, Chen B, Song Y, Zhang T, Yang W, et al. Substantial undocumented infection facilitates the rapid dissemination of novel coronavirus (SARS-CoV2). Science 2020;368(6490):489–93.

[53] Hellewell J, Abbott S, Gimma A, Bosse NI, Jarvis CI, Russell TW, et al. Feasibility of controlling COVID-19 outbreaks by isolation of cases and contacts. Lancet Glob Health 2020;8(4):e488–96.

[54] Wuhan Bureau of Statistics. Wuhan statistical yearbook 2018 [Internet]. Wuhan: Wuhan Bureau of Statistics; 2020 [cited 2020 Apr 10]. Available from: http://tjj.wuhan.gov.cn/tjfw/tjnj/202004/P020200426461240969401.pdf. Chinese.

[55] Pezzulo C, Hornby GM, Sorichetta A, Gaughan AE, Linard C, Bird TJ, et al. Sub-national mapping of population pyramids and dependency ratios in Africa and Asia. Sci Data 2017;4(1):170089.

[56] Global health security index [Internet]. London: Global Health Security Index; 2020 [cited 2020 Apr 25]. Available from: https://www.ghsindex.org/.

[57] Normile D. As normalcy returns, can China keep COVID-19 at bay? Science 2020;368(6486):18–9.

[58] Young BE, Ong SWX, Kalimuddin S, Low JG, Tan SY, Loh J, et al. Epidemiologic features and clinical course of patients infected with SARS-CoV-2 in Singapore. JAMA 2020;323(15):1488–94.

[59] Richardson S, Hirsch JS, Narasimhan M, Crawford JM, McGinn T, Davidson KW, et al. Presenting characteristics, comorbidities, and outcomes among 5700 patients hospitalized with COVID-19 in the New York City area. JAMA 2020;323(20):2052.

[60] Grasselli G, Zangrillo A, Zanella A, Antonelli M, Cabrini L, Castelli A, et al. Baseline characteristics and outcomes of 1591 patients infected with SARS-CoV-2 admitted to ICUs of the lombardy region, Italy. JAMA 2020;323(16):1574–81.

[61] Tsang TK, Wu P, Lin Y, Lau EHY, Leung GM, Cowling BJ. Effect of changing case definitions for COVID-19 on the epidemic curve and transmission parameters in Chinese mainland: a modelling study. Lancet Public Health 2020;5(5):e289–96.

[62] Chu DK, Akl EA, Duda S, Solo K, Yaacoub S, Schünemann HJ, et al. Physical distancing, face masks, and eye protection to prevent person-to-person transmission of SARS-CoV-2 and COVID-19: a systematic review and meta-analysis. Lancet 2020;395(10242):1973–87.

[63] Baker RE, Yang W, Vecchi GA, Metcalf CJE, Grenfell BT. Susceptible supply limits the role of climate in the early SARS-CoV-2 pandemic. Science 2020;369(6501):315–9.

[64] Yang J, Chen X, Deng X, Chen Z, Gong H, Yan H, et al. Disease burden and clinical severity of the first pandemic wave of COVID-19. Nat Commun 2020;11(1):5411.

[65] Mistry D, Litvinova M, Pastore y Piontti A, Chinazzi M, Fumanelli L, Gomes MFC, et al. Inferring high-resolution human mixing patterns for disease modeling. Nat Commun 2021;12(1):323.

[66] Kandel N, Chungong S, Omaar A, Xing J. Health security capacities in the context of COVID-19 outbreak: an analysis of International Health Regulations annual report data from 182 countries. Lancet 2020;395(10229):1047–53.

[67] Alegana VA, Maina J, Ouma PO, Macharia PM, Wright J, Atkinson PM, et al. National and sub-national variation in patterns of febrile case management in sub-Saharan Africa. Nat Commun 2018;9(1):4994.

[68] Huang B, Wang J, Cai J, Yao S, Chan PKS, Tam TH, et al. Integrated vaccination and physical distancing interventions to prevent future COVID-19 waves in Chinese cities. Nat Hum Behav. In press.

[69] Ge Y, Zhang W, Liu H, Ruktanonchai CW, Hu M, Wu X, et al. Effects of worldwide interventions and vaccination on COVID-19 between waves and countries. 2021. medRxiv:2021.03.31.21254702.